Functional Validation of a Common Nonsynonymous Coding Variant in *ZC3HC1* Associated With Protection From Coronary Artery Disease

Tara Linseman, MSc*; Sébastien Soubeyrand, PhD*; Amy Martinuk, MSc; Majid Nikpay, PhD; Paulina Lau, MSc; Ruth McPherson, MD, PhD

Background—Although virtually all coronary artery disease associated single-nucleotide polymorphisms identified by genome-wide association studies (GWAS) are in noncoding regions of the genome, a common polymorphism in *ZC3HC1* (rs11556924), resulting in an arginine (Arg) to histidine (His) substitution in its encoded protein, NIPA (Nuclear Interacting Partner of Anaplastic Lyphoma Kinase) is linked to a protection from coronary artery disease. NIPA plays a role in cell cycle progression, but the functional consequences of this polymorphism have not been established.

Methods and Results—Here we demonstrate that total *ZC3HC1* expression in whole blood is similar across genotypes, despite expression being slightly biased toward the risk allele in heterozygotes. At the protein level, the protective His363 NIPA variant exhibits increased phosphorylation of a critical serine residue (Ser354) and higher protein expression as compared with the Arg363 variant. Binding experiments indicate that neither SKP1 (S-phase kinase-associated protein 1) nor CCNB1 binding were affected by the polymorphism. Despite similar nuclear distribution, NIPA His363 exhibits greater nuclear mobility. NIPA suppression results in a modest reduction of proliferation in vascular smooth muscle cells, but given low proliferative capacity, a significant effect of the variant was not noted. By contrast, we demonstrate that the protective variant reduces cell proliferation in HeLa cells.

Conclusions—These findings extend the genetic association between rs11556924 and coronary artery disease risk by characterizing its effects on the encoded protein, NIPA. The resulting amino acid change Arg363His is associated with increased expression and nuclear mobility, as well as lower rates of cell growth in HeLa cells, further supporting a role for cell proliferation in atherosclerosis and its clinical consequences. **(*Circ Cardiovasc Genet*. 2017;10:e001498. DOI: 10.1161/CIRCGENETICS.116.001498.)**

Key Words: atherogenesis ■ CCNB1 ■ coronary artery disease ■ genome-wide association study ■ genomics ■ NIPA ■ phosphorylation ■ ZC3HC1

Despite the success of GWAS for coronary artery disease (CAD), the functional consequences of the majority of disease-associated variants have yet to be uncovered. In 2011, the large GWAS meta-analyses by the CARDIOGRAM (Coronary Artery Disease Genome Wide Replication and Meta-Analysis Consortium) consortium uncovered 13 novel common CAD-susceptibility loci.[1] One of the top hits in this seminal study, and the only coding single-nucleotide polymorphism (SNP), was rs11556924 found in exon 8 of *ZC3HC1*, the locus encoding NIPA (Nuclear Interacting Partner of Anaplastic Lyphoma Kinase).

See Clinical Perspective

According to 1000 Genomes data, the minor allele (T) frequency of rs11556924 ranges from 2.7% to 38% in African and European populations, respectively, with an odds ratio (OR) for CAD of 0.90 (P=2.4×10^{-17}). In addition, the few Neanderthal genomes sequenced (visualized via the UCSC Genome Browser) contain the ancestral (C) allele exclusively, indicating that this allele enrichment is unlikely the result of admixing between the 2 species but rather arose separately in Homo Sapiens.[2]

The rs11556924 polymorphism results in an amino acid change at residue 363 of NIPA, from Arg363 to His363, the recently evolved protective allele. Since the initial report of rs11556924 association with CAD,[1] the association between *ZC3HC1* and CAD has been strengthened by more recent GWAS.[3,4] Despite the robust statistical association, functional studies have yet to elucidate and substantiate the link between *ZC3HC1* and CAD, a disease with a complex etiology wherein proliferative and inflammatory components play prominent roles.[4,5]

Received May 5, 2016; accepted November 16, 2016.

From the Atherogenomics Laboratory, University of Ottawa Heart Institute, Canada.

*T. Linseman and Dr Soubeyrand contributed equally to this work.

The Data Supplement is available at http://circgenetics.ahajournals.org/lookup/suppl/doi:10.1161/CIRCGENETICS.116.001498/-/DC1.

Correspondence to Ruth McPherson, MD, PhD, Atherogenomics Laboratory, University of Ottawa Heart Institute, Ottawa, Canada K1Y 4W7. E-mail rmcpherson@ottawaheart.ca or Sebastien Soubeyrand, PhD, Atherogenomics Laboratory, University of Ottawa Heart Institute, Ottawa, Canada K1Y 4W7. E-mail ssoubeyrand@ottawaheart.ca

NIPA confers specificity to the SCF (*SKP1*, *C*ullin, *F*-Box protein)^{NIPA} complex.[6] With the addition of ROC1 (RING-finger protein 1), the complex targets CCNB1, the only known substrate of SCF^{NIPA}, to proteasome-mediated degradation. As cell cycle progresses beyond interphase, NIPA is inactivated and dissociates from the complex, resulting in the accumulation of nuclear CCNB1 and breakdown of the nuclear envelope.[6,7] By ensuring the timely presence of nuclear CCNB1, the complex contributes to the control of cell cycle progression. In late M phase/early G1, NIPA is recognized by the anaphase-promoting complex (APC/C^{cdh1}) and degraded, an event that coincides with the onset of a new round of cell division and de novo synthesis of NIPA.[8]

The geometry of the complex has been somewhat clarified. Within the SCF complex, NIPA interacts with SKP1 (S-phase kinase-associated protein 1) via its F-Box motif (amino acids 170–210).[6] Inactivation and dissociation of NIPA from the complex requires multiple phosphorylation events occurring along the CCNB1 interaction region of NIPA which spans AA352-402.[9] In that region, S354 phosphorylation seems to play a pivotal role as substituting S354 for an Ala residue results in a constitutively active NIPA.

The Arg363His substitution is within a highly conserved region of the protein and represents a significant change from a positively charged aliphatic side chain to a more neutral imidazole ring and is predicted to have a damaging effect by Polyphen-2 (http://genetics.bwh.harvard.edu/pph2/). However, the consequences on NIPA function are likely to be minor because both alleles are prevalent, at least in the European population.

Methods

For additional Methods information, please refer to the Expanded Methods section in the Data Supplement.

Cell Culture and Treatments

HeLa and HEK-293T cells were cultured and maintained at 5% CO_2 in Dulbecco's Modified Eagle Medium (Life Technologies), containing 4.5 g/L glucose, and supplemented with 10% fetal bovine serum, 1% L-glutamine, and 1% penicillin–streptomycin (Life Technologies). Human thoracic smooth muscle cells were obtained from Dr J.G. Pickering (Lot HITC6) and maintained in supplemented SmGM-2 media (Lonza). Human umbilical vein epithelial cells (HUVECs) were grown in modified F-12K as suggested by the supplier (ATCC).

Western Blotting

Proteins (30 μg) were resolved by SDS-PAGE, transferred to nitrocellulose membranes, and subjected to detection with cognate antibodies.

Cloning and Expression Constructs

Please refer to the Expanded Methods section in the Data Supplement for details.

Fluorescence Recovery After Photobleaching

Plasmids spanning NIPA variants with an N-terminally enhanced yellow fluorescent protein were transfected for 24 hours in HEK-293T using Fugene 6. Ten randomly distributed cells expressing comparable, intermediate levels of yellow fluorescent protein-NIPA (as assessed by yellow fluorescent protein intensity) were scored per construct per experiment. Each cell was subjected to 2 rounds of fluorescence recovery after photobleaching/acquisition for a total of 20 determinations per construct. Bleaching was performed for 1.2 s (48 iterations) using an Argon laser 515 nm emission line at 35% laser intensity over a 20 μm^2 surface of the nucleus. Fluorescence recovery was then plotted as a function of time (26 ms acquisitions for a total time of 2500 ms) over a 4 μm^2 surface and fit to a logarithmic best-fit regression using the Miscrosoft Excel software; time required to reach 50% of the maximal value post-fluorescence recovery after photobleaching was calculated from the resulting equation.

ZC3HC1 mRNA Expression

Human Studies

The study was approved by the Human Ethics Experimentation Committee of the University of Ottawa Heart Institute, and written informed consent was obtained from all participants.

Total mRNA Expression

RNAs were isolated from extracted whole blood samples of 158 healthy patients and reverse-transcribed as described previously.[10] Primers for *ZC3HC1* and PPIA (peptidylprolyl isomerase A) were used to determine the relative amount of *ZC3HC1*; relative copy numbers of *ZC3HC1* transcripts were normalized to the expression levels of PPIA. Quantitative polymerase chain reaction was performed using a LightCycler 480 II instrument and the LightCycler 480 software (Roche).

Allele-Specific Expression Analysis

Data acquisition was performed on a LightCycler 480 (Roche) using an rs11556924 TaqMan-specific probe (Thermo Fisher). A standard curve was generated by using dilutions of homozygote DNA samples. A total of 75 healthy heterozygote controls were analyzed (73 shared with analysis above). Sample and standard curve values were log-transformed to fit a linear relationship. Analyses of raw data were performed using Microsoft Excel.

Cell Proliferation Assay

Cell proliferation was quantified using the WST-1 assay. HeLa cells were seeded at ≈30 000 cells/ well in 24-well culture plates and were left to grow overnight at 37°C at 5% CO_2. Cells (6 wells per condition) were transfected with 0.5 μg of DNA per well using Fugene 6 transfection reagent. For HUVEC and vascular smooth muscle cells (VSMC), cells at ≈70% density were infected with comparable titers of viral particles, as assessed by quantitative reverse transcriptase polymerase chain reaction quantification of PLVX in the viral suspension. After 72 hours, media was removed and replaced with media supplemented with Premix WST-1 Cell Proliferation Reagent (TaKaRa; 100 μL WST-1 reagent/1 mL media). This widely used proliferation assay was selected for its robustness and reproducibility, an important consideration when small differences among tested samples are expected. A limitation to this assay is that it is not measuring cell number directly but metabolic activity, which, everything else being equal, is proportional to cell number. Cells were incubated for 1 hour at 37°C at 5% CO_2. Two wells without cells were used for background absorbance readings. Absorbance was measured at 460 nm on the Synergy MX BioTek plate reader

Binding Assays

Pull-down assays were performed on HEK-293T cell lysates transfected with either CCNB1 or FLAG-NIPA for 48 hours. Cells were lysed in buffer A and cleared by centrifugation (1 minute at 21 000*g*). The supernatant (400 μg of protein) was incubated with the appropriate bait (GST-SKP1 or GST-NIPA) for either 1 (SKP1) or 2 hours (NIPA) with rotation. For SKP1, pull-down conditions were in buffer A, whereas for CCNB1 binding, the supernatant was first diluted 10× in buffer B (25 mmol/L Tris-HCl, 50 mmol/L NaCl, 0.25% Nonidet P40, 0.5 mmol/L EDTA) and recentrifuged for 1 minute at 21 000*g*. On completion of binding, samples were washed 3× with either buffer A or B (without inhibitor supplements) for SKP1 and CCNB1 pull-downs, respectively.

Statistical Methods

Differences between sample groups were tested for statistical significance using nonpaired, 2-tailed Student's *t* tests, which was chosen

over nonparametric testing to (1) better capture quantitative differences across the samples, (2) for its greater statistical power, and (3) for consistency with the published literature, where it is abundantly used to test small sample sizes. A drawback is that normality has to be assumed, which although reasonable cannot be established for small sample sizes. To address this, the same data points were subjected to nonparametric tests using the Mann–Whitney U Test, which confirmed statistically significant differences ($P<0.05$) observed with the *t* test in all experiments involving >3 samples. For experiments involving 3 samples, a *P* value of 0.064 was obtained, regardless of the extent of the differences observed, likely because the Mann–Whitney U Test lacks statistical power and is insensitive to effect size.

Epistasis Analysis

Gene coordinates based on GRCh37/hg19 were obtained from BioMart-Ensembl. Epistasis analysis was performed using PLINK (v1.07) software in a sample of genetically unrelated 4535 cases and 2977 controls of White ancestry who were genotyped at the University of Ottawa Heart Institute. Prior to epistasis analysis, we pruned SNPs and kept only those in linkage equilibrium (linkage disequilibrium $r^2 < 0.2$). The epistasis test uses the logistic regression and makes a model based on allele dosage for each SNP, A and B, and fits the model

$$Y = \beta_0 + \beta_1 A + \beta_2 B + \beta_3 AB + \varepsilon. \quad (1)$$

From this model, PLINK computes β_3 and corresponding standard error. The OR of interaction is calculated as

$$\text{OR of interaction} = \exp(\beta_3). \quad (2)$$

The allelic OR corresponding to each allele count stratum, its standard error, and 95% confidence interval are calculated using the following equation:

$$\text{Allelic OR} = \frac{ad}{bc}, \quad (3)$$

where *a* is the minor allele count in cases, *b* is the minor allele count in controls, *c* is the major allele count in cases, and *d* is the major allele count in controls,

with the standard error of the log OR being

$$\text{SE}\{\ln(\text{OR})\} = \sqrt{\frac{1}{a}+\frac{1}{b}+\frac{1}{c}+\frac{1}{d}}, \quad (4)$$

and 95% confidence interval of OR is given by

$$\text{Lower limit of 95\% CI} = \exp\left(\ln(\text{OR}) - \text{SE}\{\ln(\text{OR})\}\right) \quad (5)$$

$$\text{Upper limit of 95\% CI} = \exp\left(\ln(\text{OR}) - \text{SE}\{\ln(\text{OR})\}\right). \quad (6)$$

Results

Effects of rs11556924 on *ZC3HC1* mRNA Expression in Peripheral Blood Mononuclear Cells

Analysis of the linkage disequilibrium structure of the *ZC3HC1* gene from the 1000 Genomes data indicates that rs11556924 is the only strongly CAD-associated SNP (Figure I in the Data Supplement). The original study failed to identify rs11556924 as an expression quantitative locus for *ZC3HC1*, suggesting that the polymorphism did not affect transcript abundance. We first elected to validate this observation given that SNPs located in exons tend to be expression quantitative loci.[11] mRNA expression analyses were performed on whole blood RNA from healthy individuals to avoid confounders related to disease processes or medication. Using a cohort of 160 control subjects that were clustered according to their genotypes, NIPA transcript abundance was assessed by quantitative reverse transcriptase polymerase chain reaction in peripheral blood mononuclear cells, which exhibit abundant expression of *ZC3HC1* (Figure 1A). After correction for the housekeeping gene *PPIA*, no significant difference in *ZC3HC1* expression was observed across the genotypes.

The absence of statistical significance might have reflected a genuine similarity across the genotypes or insufficient statistical power. This was addressed by measuring the relative levels of the allelic transcripts within each heterozygote patient, reasoning that the T allele might show reduced expression. TaqMan analysis revealed that the T allele was indeed expressed at a slightly lower level (43±2%) in heterozygotes (Figure 1B). In summary, these findings point to a mild allelic imbalance in heterozygotes, favoring the risk allele, but to no net change in total *ZC3HC1* across genotypes.

His363 Reduces Proliferation of HeLa Cells

Next, we turned our attention to the encoded protein, NIPA. The rs11556924 polymorphism results in either a histidine or an arginine at position 363 of NIPA. To examine the functional impact of the NIPA Arg363His variant, constructs encoding FLAG-tagged NIPA of either variant were generated and their impact on cellular proliferation assessed. HeLa cells were

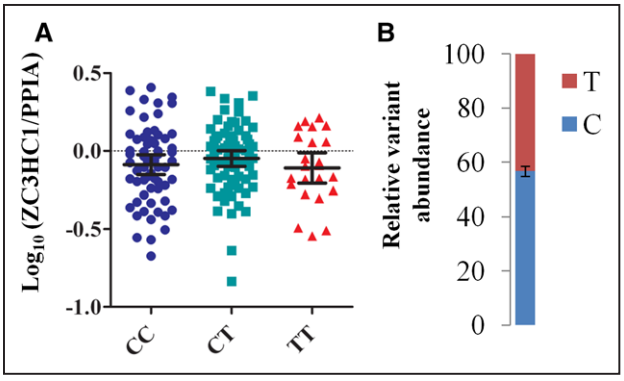

Figure 1. *ZC3HC1* expression in whole blood. **A**, Whole blood RNA was extracted from human control patients, and levels of *ZC3HC1* and *PPIA* (peptidylprolyl isomerase A; housekeeping gene) mRNA were measured by qRT-PCR. *ZC3HC1* levels were then normalized to the levels of PPIA. Values were Log_{10} transformed and plotted as a function of genotype. Genotypes (patient numbers): CC=R363 variant (62); CT=heterozygote (73); TT=H363 variant (23). Bars represent averages±95% confidence intervals (α=0.05). No statistically significant differences were seen across the 3 groups (1-way ANOVA), irrespective of logarithmic transformation. **B**, Allele-specific expression analysis. Expression of each variant of *ZC3HC1* in 75 control heterozygote subjects was determined by TaqMan. Error bars represent SD. C indicates reference allele; CAD, coronary artery disease; qRT-PCR, quantitative reverse transcriptase polymerase chain reaction; and T, CAD-protective allele.

chosen because (1) they were previously used to demonstrate that NIPA suppression was associated with early mitotic entry and (2) HeLa proliferation requires CCNB1.[6,12] This earlier study did not address the consequences of NIPA silencing on HeLa proliferation. To ensure HeLa could be used to study NIPA functionally in this type of assay, NIPA was suppressed using NIPA-specific siRNAs, and cellular proliferation was measured using the WST-1 assay. NIPA suppression led to an ≈20% increase in WST-1 signal, consistent with increased cell proliferation over 48 hours, indicating that HeLa cells represent a valid model to study NIPA function (Figure 2A).

The impact of NIPA overexpression was examined next. Both variants (H363 or R363) were separately introduced in HeLa cells by transient transfection of FLAG-tagged constructs (Figure 2B, top). Interestingly, the variants had contrasting effects. Although transfection of the protective (H363) variant resulted in a slight decrease in proliferation, introduction of the R363 increased it to a similar extent. Western blots confirmed that both forms were expressed at similar levels (Figure 2B, bottom).

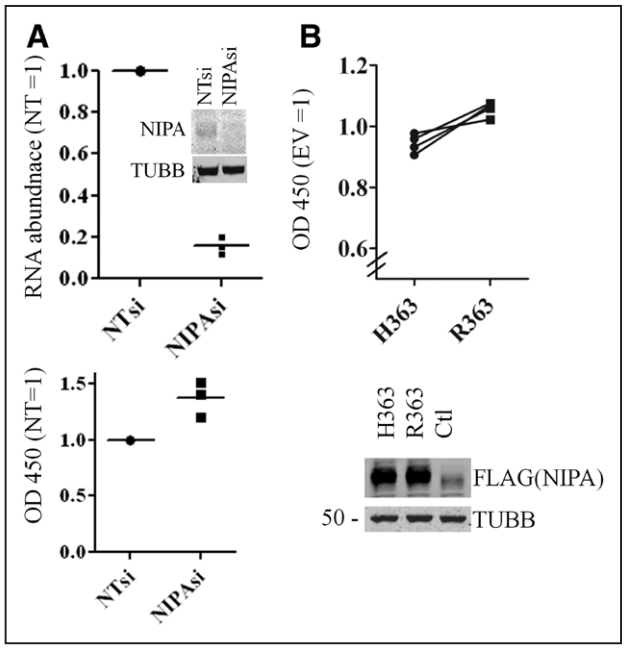

Figure 2. Introduction of the protective variant leads to reduced proliferation in HeLa cells. **A**, *ZC3HC1* suppression promotes HeLa proliferation. siRNA was performed for 48 h with a *ZC3HC1*-targeting siRNA, and cell proliferation was measured using the WST-1 assay. **Top**, Corrected *ZC3HC1* mRNA abundance (relative to *PPIA* [peptidylprolyl isomerase A]), normalized to the NTsi values. Inset, Western blot of NIPA in nuclear fractions. **Bottom**, Proliferation measured under conditions described in **A**. Difference is statistically significant ($P<0.05$, 2-tailed *t* test Student's *t* test). Individual normalized values and corresponding averages are shown. **B**, Impact of *ZC3HC1* transfection on proliferation. **Top**, Cell proliferation was estimated using the WST-1 assay 72 h after transfection with either variant. Values represent 4 biological replicates and are normalized to empty vector; matched biological replicates are connected by a line. H363 transfection resulted in reduced proliferation by 6% (vs empty vector [EV]; $P=0.03$), while R363 transfection increased it by the same amount ($P=0.02$). In each biological replicate, the H363 variant reduced proliferation by 16% vs R363 (0.84±0.038 (95% CI); $P=5.8\ E^{-6}$, Student's 2-tailed *t* test). **Bottom**, NIPA expression control. Cells from **B** were lysed on completion of the proliferation assay and analyzed by Western blotting. FLAG-NIPA migrates as an ≈ 65 kDa band. NIPA, Nuclear Interacting Partner of Anaplastic Lyphoma Kinase

Overexpression of NIPA Increases CCNB1 Levels in HeLa Cells

One possible explanation for differential effects of the 2 variants on cell proliferation could involve altered CCNB1 degradation. Indeed, CCNB1 levels are affected by NIPA: NIPA suppression was shown to increase the amount of CCNB1.[6] Moreover, the CCNB1 interaction epitope on NIPA is located within AA353-402.[9] We hypothesized that H363 transfection should lead to decreased CCNB1 levels that may account for the reduced proliferation. To test the relative ability of NIPA to promote CCNB1 degradation, levels of CCNB1 were measured by Western blot in the same HeLa cell lysates that were tested previously for proliferation. Surprisingly, both variants increased CCNB1 mildly albeit to the same extent (Figure II in the Data Supplement). Thus, although changes in CCNB1 levels were observed, they are unlikely to account for the contrasting effects on proliferation.

Proliferation Is Reduced by NIPA Suppression but Unaffected by NIPA Overexpression in VSMC and HUVEC

Although NIPA is required to regulate HeLa proliferation, its role in primary cells is unresolved. To start addressing the contribution of NIPA to model systems more pertinent to cardiovascular disease, NIPA expression was suppressed in VSMC and HUVEC models. In both systems, reduced NIPA resulted in a significant albeit modest ≈10% decrease in proliferation (Figure 3A). Having established that NIPA contributes to the proliferation of both cell types, the impact of each NIPA variant was next examined via lentiviral delivery; this approach was chosen to overcome transfection efficiency hurdles inherent to these cells. Infection resulted in a strong expression of both variants, as assessed by Western blot (Figure 3B). However, no associated changes in proliferation were observed.

Genetic Epistasis Between *ZC3HC1* With *CCNB1* in CAD

The lack of differential impact of NIPA on CCNB1 observed in HeLa cells was unexpected and suggested that the *ZC3HC1* gene product might regulate cell proliferation and CAD risk via other mechanisms. Because CCNB1 is a well established partner of NIPA and a major regulator of cell cycle regulation, we performed an epistasis screen between *ZC3HC1* and all genes populating the Reactome R-HSA-69278.1 data set, a curated list of 321 genes, which includes *CCNB1*, involved in mitosis and cell cycle regulation. After pruning, the resulting list included 1134 independent ($r^2<0.2$) SNPs, which were interrogated for possible epistasis with *ZC3HC1*. The analysis revealed 50 independent SNPs to be nominally associated with *ZC3HC1*, of which, notably, *CCNB1* was the most strongly associated ($P=0.001372$; Table; Table I in the Data Supplement). Although statistical significance was lost after correction for multiple testing, these data are consistent with *ZC3HC1* and *CCNB1* playing a concerted role in the development of CAD.

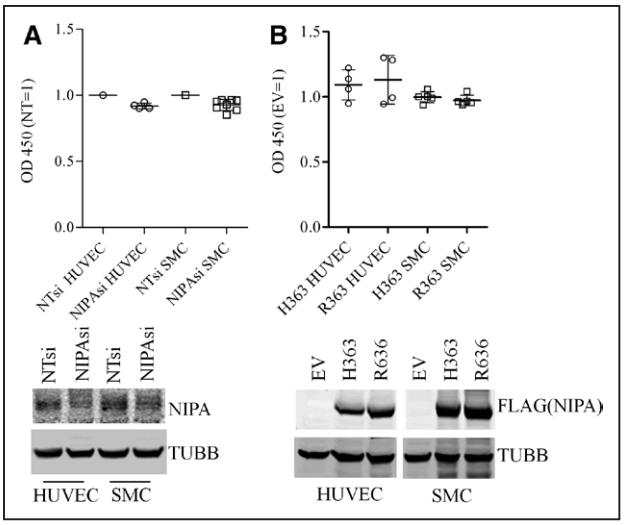

Figure 3. Proliferation is reduced by NIPA suppression but unaffected by NIPA overexpression in SMC and HUVEC. Individual experimental results and averages (±SD) are shown. A Western blot confirming suppression of NIPA and overexpression of NIPA is shown below each proliferation graph. **A**, Knockdown (72 h) resulted in 43% (±0.11SD) and 25% (±0.06 SD) of control (NTsi treated) NIPA RNA level for human smooth muscle cells (SMC; n=8) and human umbilical vein cells (HUVEC; n=4), respectively. Both NIPAsi treatments were statistically significantly different from the nontarget (NT) control (Student's *t* test, $P<0.05$). **B**, Overexpression of NIPA. NIPA was transduced in SMC and HUVEC with lentiviruses. No statistically significant impact on proliferation was observed, as compared to empty virus infections (EV). NIPA indicates Nuclear Interacting Partner of Anaplastic Lyphoma Kinase.

Interaction With CCNB1 and SKP1 Is Not Altered by Arg363His Substitution

To further test a possible functional CCNB1/NIPA interaction, the effect of the polymorphism on the interaction between CCNB1 and NIPA was assessed by using a region on NIPA that was shown to be necessary and sufficient for its interaction with CCNB1 (AA353-402).[9] Lysates of HEK-293T cells overexpressing *CCNB1* were incubated with either form of GST-coupled NIPA, and bound CCNB1 was recovered and quantified by Western blot (Figure 4A**).** There was no significant difference in the ability of either form of NIPA to enrich CCNB1, suggesting that binding to CCNB1 is unaffected by the polymorphism.

Inactivation of NIPA involves its dissociation from the SCF complex in G2/M. More specifically, the interaction between NIPA and SKP1 is lost, presumably as a means to fully inactivate the complex and prevent spurious degradation of CCNB1.[6] Although the region responsible for the interaction of NIPA with SKP1 (AA170-210) is some distance from residue 363, it remained possible that the mutation introduces long distance changes either in *cis* or *trans* (eg, regulatory post-transcriptional modifications). To test the ability of SKP1 to interact with either form, GST-SKP1 was expressed in *Escherichia Coli*, bound to GST beads and incubated with either form expressed in HEK-293T cells, followed by the isolation of the bound material. Western blotting of the pull-downs revealed similar amounts of both variants, indicating that the polymorphism is unlikely to affect the ability of NIPA to interact with SKP1.

Increased Protein Expression of the Protective NIPA His363 Variant

During the proliferation assays, we noted that the protective variant tended to be expressed at ≈10% higher levels, although the difference was not statistically significant over 4 determinations. Because NIPA expression is likely to contribute to its function, the possibility that the polymorphism leads to distinct expression levels was directly tested. Constructs expressing either variant in tandem with GFP via an internal ribosome entry site were designed and introduced in HeLa cells; the ratio of NIPA to GFP was then measured by Western blot. Consistent with our earlier results, we did observe that protein levels of the H363 variant surpassed those of the R363 allele by ≈15% (Figure 5). This difference persisted even when the absolute expression level of NIPA was changed by varying the amount of expression plasmid transfected.

Phosphorylation at Ser354 Is Reduced in the Arg363 Risk Variant

Interestingly, we observed that the His363 form extracted from HeLa cells tended to display ≈1 kDa retardation by Western blot when compared with the Arg363 form, suggesting that

Table. Allele Counts and Corresponding Odds Ratios (OR) for Various Combinations of rs11556924 and rs2069433 Genotypes

rs11556924 Genotype	CAD Status	rs2069433 Allele Counts C	rs2069433 Allele Counts T	OR of CAD for rs2069433 (T allele)	95% CI	OR of Interaction
TT	Cases	44	476	0.76	0.49–1.16	OR=1.51; P=0.0014
	Controls	47	671			
TC	Cases	130	1492	0.91	0.71–1.17	
	Controls	144	1812			
CC	Cases	79	1361	1.57	1.18–2.1	
	Controls	129	1413			

Significant enrichment of the rs2069433-T allele in the risk population (cases). Odds ratio of developing CAD in the population carrying the homozygous protective phenotype rs11556924-TT (versus CC): 0.78 (95% CI 0.68–0.89). CAD indicates coronary artery disease; CI, confidence interval; and OR, odds ratio.

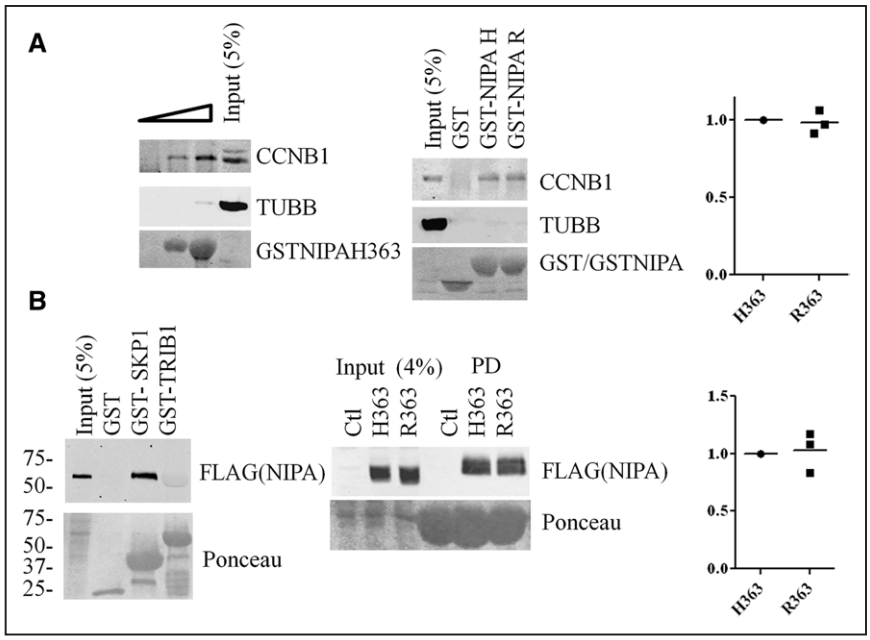

Figure 4. Binding to CCNB1 and SKP1 is unaffected by the polymorphism. **A**, CCNB1 binding to a GST fusion peptide encompassing AA353-402 of NIPA. Pull-downs were performed on HEK-293T cells transiently overexpressing CCNB1 and analyzed by Western blotting. **Left**, Titration with increasing GST-H363 fusion bait. **Middle**, Binding to GST-NIPA H and R. **Right**, Quantification of the binding, relative to the amount of bait and normalized to H363. Values from 3 distinct binding assays (representing a total of 14 technical replicates) with their means±SD are shown. **B**, Binding of NIPA to GST-SKP1. **Left**, Specific binding of NIPA to GST- SKP1. Pull-down assays of HEK-293T cells transfected with NIPA (H363) by GST-SKP1, GST, and GST-TRIB1, a control protein, analyzed by Western blot. **Middle**, Binding of SKP1 to both forms (expressed in HEK-293T) is similar. Ponceau staining of the blot corresponding to GST-SKP1 is shown below. **Right**, Quantification of 3 distinct binding assays as performed in **A**. NIPA indicates Nuclear Interacting Partner of Anaplastic Lyphoma Kinase.

phosphorylation of NIPA might be affected. Alternatively, this shift may have been because of charge or structural constraints that persist despite denaturation. Additional experiments confirmed this finding in HeLa cells, particularly visible on lower percentage (≤8% gels; see Figure III in the Data Supplement). NIPA cycles through rounds of activation and inactivation involving phosphorylation events that dissociate NIPA from the SCF complex.[6] Chief among this phosphorylation cascade, Ser354 plays a critical role in promoting disassembly of the complex: a Ser354A mutation leads to a constitutively active enzyme that degrades CCNB1 continuously.[13] The relative proximity of Arg363 versus His363 to this key residue suggested that rs11556924 may regulate NIPA function by differentially affecting Ser354 phosphorylation. To test this hypothesis, plasmids encoding the 2 forms of NIPA were transfected in HeLa cells, and the phosphorylation at Ser354 was assessed using a phosphoSer354-specific antibody by Western blot. Importantly, pilot titration experiments indicated that Ser354 phosphorylation was inversely proportional to the amount of NIPA introduced (Figure IV in the Data Supplement). Over 6 independent replicates, Arg363 was consistently less modified (versus His363) on Ser354 (by 5% on average; Figure 6), despite being expressed at a slightly lower level.

Arg363 and His363 Display Indistinguishable Cellular Distribution

We next examined the cellular distribution of NIPA by immunocytochemistry. NIPA nuclear localization signal (Ser401-415) is further C-terminal but reasonably close to Ser363 as to affect its cellular distribution. When expressed as FLAG-tagged versions, both forms were localized exclusively in the nucleus in interphase cells (Figure 7A). Indeed, both forms displayed pan-nuclear presence with some perinuclear enrichment in HeLa cells, as seen previously.[6] To capture possibly subtle differences between the 2 forms, the variants were tagged with either CFP or GFP and coexpressed in HeLa cells, where both signals were found to overlap perfectly (Figure 7B), indicating that the two forms localize to the same subnuclear regions.

Enhanced Nuclear Mobility of the His363 Variant

Although there was no evidence of localization differences in the steady state, we sought to determine whether the 2 variants

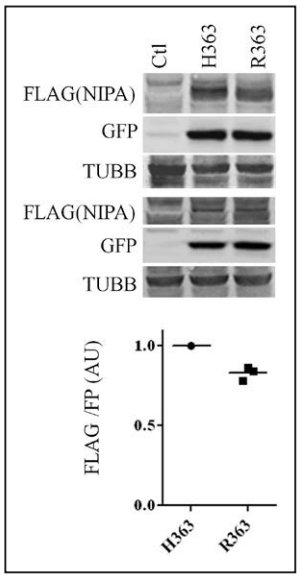

Figure 5. Reduced expression levels of the risk variant. HeLa cells were transfected using GenJet II for 48 h with bicistronic plasmids encoding either NIPA variant in tandem with GFP. Cells were than lysed and analyzed by Western blotting using antibodies directed against GFP and FLAG. Ratios of NIPA to GFP signals were calculated for each technical replicate and values averaged over 4 technical replicates per experiment. Two representative blots, with variable FLAG-NIPA expression levels obtained by using either 1 μg or 0.5 μg of DNA per transfected well, are shown. Quantifications of 3 biological replicates are shown. Values are normalized to the H363 variant (set to 1). Difference is statistically significant (Student's 2-tailed *t* test; *P*=0.02). NIPA indicates Nuclear Interacting Partner of Anaplastic Lyphoma Kinase.

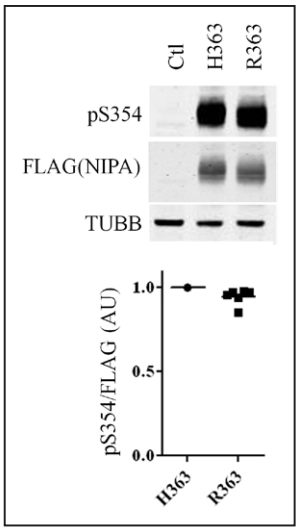

Figure 6. Reduced NIPA S354 phosphorylation in the risk variant expressed in HeLa cells. Relative phosphorylation at S354 was assessed by Western blotting of extracts of HeLa cells. **Top**, Typical gel; and **bottom**, quantification of 6 biological replicates, normalized to H363 (±95% CI). Ctl, pCDNA3. Difference (5.3%) is statistically significant (Student's 2-tailed *t* test; *P*=0.044). NIPA indicates Nuclear Interacting Partner of Anaplastic Lyphoma Kinase.

exhibit kinetic differences. The kinetics of both variants were assessed by fluorescence recovery after photobleaching experiments performed in HEK-293T cells; both variants were first tagged with the same fluorescent protein species to minimize the possible confounder of using different FP species. Interestingly, although both variants displayed kinetics that overlapped largely in any given experiment as shown by the overlapping standard deviations, the H363 variant was significantly faster, on average, with a half-time of recovery shortened by ≈9% (Figure 8).

Discussion

Despite the success of recent GWAS, there has been limited progress in understanding the function of the multiple risk loci identified. Here we have interrogated the functional effects rs11556924 encoding a nonsynonymous variant in *ZC3HC1*. This is 1 of only 2 missense polymorphisms among the 202 false discovery rate $q<0.05$ variants recently associated with CAD.[4] The presence of a disease-associated SNP within *ZC3HC1*, while strongly suggestive, does not establish that the function of the encoded protein, NIPA, is altered.

Indeed, rs11556924 has been shown to affect the expression of neighboring *KLHDC10* (Kelch domain-containing protein 10), suggesting that *KLHDC10* rather than *ZC3HC1* may be the causal CAD gene.[1,14] KLHDC10 is a recently characterized protein that promotes oxidative stress–induced cell death.[15] Although the contribution of this protein to CAD remains unclear, its involvement in apoptosis is consistent with the processes underlying plaque formation.[16] Comparing the expression levels of KLHDC10 between CAD and control cohorts should help clarify this point.

Interestingly, we observed that *ZC3HC1* was subject to a modest allelic imbalance favoring the risk allele in heterozygous individuals. Allelic imbalance, preferential expression of an allele in diploid organisms, is a fairly common phenomenon.[17–19] Thus, the risk allele seems to show greater expression despite the fact that no coherent genotypic impact on whole blood expression level (CC>CT>TT) was evident. Similarly, previous studies have failed to identify rs11556924 as an expression quantitative locus for *ZC3HC1* expression.[1,20] However, the significant heterogeneity in *ZC3HC1* levels observed may obscure subtle effects that a larger cohort study may uncover.

Cardiovascular disease is to a large extent a proliferative disease, although the role proliferation plays therein is as complex as the disease itself.[21] Using a HeLa cell model, we demonstrate that the protective variant imparts a net proliferative disadvantage, while the more common risk variant promotes proliferation. By contrast, no proliferation effects were detectable in VSMC or HUVEC model systems. Yet, a 10% reduction in proliferation was observed on NIPA suppression, emphasizing that (1) maximal proliferation of VSMCs and HUVEC requires NIPA, and (2) our ability to assess NIPA function in those 2 cell types is limited. The limited impact on proliferation may reflect the relatively slow growth of both cell types, which we approximate at ≈2 days for HUVEC and ≈3 days for smooth muscle cells, for which low residual NIPA levels may suffice. Accordingly, under the experimental conditions used, the 10% proliferative window that depends on NIPA may not be sufficiently large to allow for the detection of changes associated with the introduction of NIPA variants. Another limitation to these findings is that proliferation was quantified using the WST-1 assay, which ultimately measures

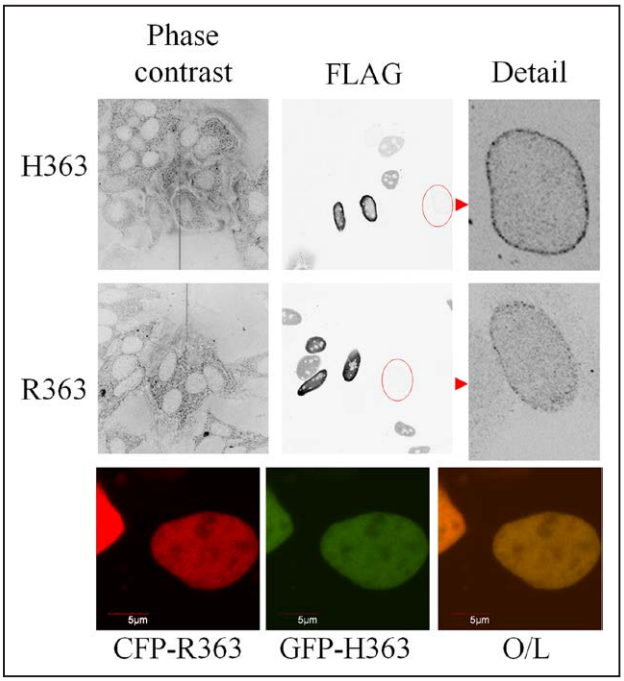

Figure 7. NIPA variants show similar nuclear distribution. **A**, FLAG-NIPA variants transfected in HeLa cells were revealed by immunocytochemistry using a FLAG-specific antibody. Details (darkened) of 2 cells expressing lower levels of NIPA (circled) are singled out to the right to highlight the nuclear distribution of NIPA. **B**, The 2 NIPA variants were expressed as either N-terminal GFP or CFP fusions in HEK-293T cells and visualized by confocal microscopy using the appropriate channels. Cells were fixed 24 h post-transfection. NIPA indicates Nuclear Interacting Partner of Anaplastic Lyphoma Kinase.

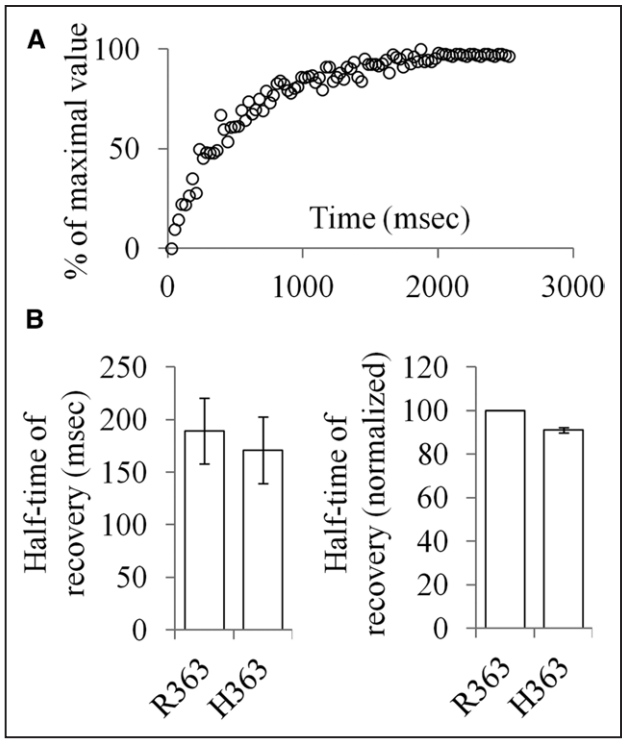

Figure 8. Enhanced nuclear mobility of the protective variant revealed by FRAP analyses. Fusion proteins consisting of EGFP fused to either form of NIPA were transfected into HEK-293T cells and subjected to fluorescence recovery after photobleaching (FRAP). **A**, Typical recovery profile (H363 variant is shown). **B**, The H363 displays faster kinetics. Twenty determinations per construct were performed for each experiment. **Left**, Data are shown for a typical experiment (±SD); and **Right**, expressed as the mean of 3 independent experiments, normalized to R363 (±SD). Differences were statistically significant (2-tailed Student *t* test; $P<0.01$). NIPA indicates Nuclear Interacting Partner of Anaplastic Lyphoma Kinase.

cell metabolism rather than cell numbers, and the possibility exists that our methodologies are affected by cell viability.

Among a subset of genes involved in cell cycle control, *CCNB1* showed the strongest genetic association with *ZC3HC1* and CAD. In light of the well-established interplay between CCNB1 and NIPA at the protein level, albeit in non-CAD contexts, the genetic evidence of a convergence of *ZC3HC1* and *CCNB1* strongly supports a causal role for NIPA on CAD, by functionally linking rs11556924 to CCNB1. This nominally significant genetic association will benefit from a targeted replication in additional CAD/control cohorts because it did not achieve statistical significance after Bonferroni correction. These results do not exclude the possibility that rs11556924 exhibits pleiotropic effects, and NIPA-independent contributions (eg, *KLHDC10*) have to be considered.

Although this article was in revision, work by Jones et al[22] reinforcing the interaction between *CCNB1* and rs11556924 was published. Using isogenic adenocarcinoma cell lines, the authors demonstrate that the risk allele is associated with a slower CCNB1 nuclear accumulation, increased total CCNB1, as well as a higher mitotic index, although, unexpectedly, without proliferation changes. These results contrast with our findings demonstrating increased proliferation with the risk variant in HeLa cells. These disparities, which probably reflect cell type background or expression level differences, reinforce the need to revisit these findings in the context of untransformed cells and the endogenous locus.

The R-H substitution at residue 363 would be expected to modify the tertiary structure of the protein, which could in turn alter phosphorylation of secondary sites (eg, Ser359 and Ser395). Unfortunately, structural information on NIPA is currently lacking. Nevertheless, the region is Ser- and Pro-rich and predicted to be largely unstructured according PsiPred (http://bioinf.cs.ucl.ac.uk/psipred/) and, thus, readily accessible to modifying enzymes and other interactors. Further pointing to structural differences, fluorescence recovery after photobleaching analyses revealed that the Arg-His substitution leads to increased mobility. Greater mobility could reflect a more transient inclusion within a higher molecular complexes (eg, SCF complex), but this seems unlikely as recombinant NIPA was overexpressed and present in excess stoichiometry in comparison with the rest of the SCF complex; hence, these measurements are expected to largely quantify the unassociated pool. Rather, the different mobilities further underscore structural differences between the 2 forms, either as a direct result of the mutation or as the result of differential post-translational modifications.

By design, this study was focused on HeLa cells, largely for practical reasons: HeLa cells are well characterized, are readily transfectable, and are generally amenable to experimental investigations. Importantly, HeLa proliferation depends on both NIPA and CCNB1,[6,12] indicating that the NIPA axis therein is at least partially functional. Clearly, the HeLa model is adequate as a cell biology tool to study NIPA but insufficient to study its contribution of the complexity of CAD, which involves the concerted contributions of multiple cell types in a proinflammatory milieu.[16] Although our attempts at measuring the impacts of the NIPA variants in VSMC and HUVEC did not detect differences between both variants, a contribution of NIPA to proliferation was indeed observed.

Together with the recently published report of Jones et al,[22] this study strengthens the link between *ZC3HC1* and CAD and form the basis for follow-up experiments to be performed in the context of models of atherosclerosis. This could be achieved by establishing stable isogenic CAD-relevant cell lines specifically edited for R363H (eg, via CRISPR/*Cas*9), but ultimately experiments involving whole animals will be required. In this regard, one important factor to consider is the subtle effect of NIPA R363H on CAD risk, which may be difficult to detect in the background of murine models of atherosclerosis.

Acknowledgments

We are grateful to Dr Florian Bassermann for providing us with the pcDNAFLAG-NIPAR363 expressing construct. We also thank Dr Lena Illert for providing us with a GST-NIPA fusion plasmids and for her constructive inputs. We are also grateful to Mike Seto for performing early experiments not included in this article.

Sources of Funding

This work was funded by the Heart & Stroke Foundation of Canada T-7268.

Disclosures

None.

References

1. Schunkert H, König IR, Kathiresan S, Reilly MP, Assimes TL, Holm H, et al.; Cardiogenics; CARDIoGRAM Consortium. Large-scale association analysis identifies 13 new susceptibility loci for coronary artery disease. *Nat Genet*. 2011;43:333–338. doi: 10.1038/ng.784.
2. Green RE, Krause J, Briggs AW, Maricic T, Stenzel U, Kircher M, et al. A draft sequence of the Neandertal genome. *Science*. 2010;328:710–722. doi: 10.1126/science.1188021.
3. Dichgans M, Malik R, König IR, Rosand J, Clarke R, Gretarsdottir S, et al.; METASTROKE Consortium; CARDIoGRAM Consortium; C4D Consortium; International Stroke Genetics Consortium. Shared genetic susceptibility to ischemic stroke and coronary artery disease: a genome-wide analysis of common variants. *Stroke*. 2014;45:24–36. doi: 10.1161/STROKEAHA.113.002707.
4. Nikpay M, Goel A, Won HH, Hall LM, Willenborg C, Kanoni S, et al.; CARDIoGRAMplusC4D Consortium. A comprehensive 1,000 Genomes-based genome-wide association meta-analysis of coronary artery disease. *Nat Genet*. 2015;47:1121–1130. doi: 10.1038/ng.3396.
5. Andrés V. Control of vascular cell proliferation and migration by cyclin-dependent kinase signalling: new perspectives and therapeutic potential. *Cardiovasc Res*. 2004;63:11–21. doi: 10.1016/j.cardiores.2004.02.009.
6. Bassermann F, von Klitzing C, Münch S, Bai RY, Kawaguchi H, Morris SW, et al. NIPA defines an SCF-type mammalian E3 ligase that regulates mitotic entry. *Cell*. 2005;122:45–57. doi: 10.1016/j.cell.2005.04.034.
7. Bassermann F, Peschel C, Duyster J. Mitotic entry: a matter of oscillating destruction. *Cell Cycle*. 2005;4:1515–1517. doi: 10.4161/cc.4.11.2192.
8. Klitzing Cv, Huss R, Illert AL, Fröschl A, Wötzel S, Peschel C, et al. APC/C(Cdh1)-mediated degradation of the F-box protein NIPA is regulated by its association with Skp1. *PLoS One*. 2011;6:e28998. doi: 10.1371/journal.pone.0028998.
9. Bassermann F, von Klitzing C, Illert AL, Münch S, Morris SW, Pagano M, et al. Multisite phosphorylation of nuclear interaction partner of ALK (NIPA) at G2/M involves cyclin B1/Cdk1. *J Biol Chem*. 2007;282:15965–15972. doi: 10.1074/jbc.M610819200.
10. Douvris A, Soubeyrand S, Naing T, Martinuk A, Nikpay M, Williams A, et al. Functional analysis of the TRIB1 associated locus linked to plasma triglycerides and coronary artery disease. *J Am Heart Assoc*. 2014;3:e000884. doi: 10.1161/JAHA.114.000884.
11. Veyrieras JB, Kudaravalli S, Kim SY, Dermitzakis ET, Gilad Y, Stephens M, et al. High-resolution mapping of expression-QTLs yields insight into human gene regulation. *PLoS Genet*. 2008;4:e1000214. doi: 10.1371/journal.pgen.1000214.
12. Yuan J, Yan R, Krämer A, Eckerdt F, Roller M, Kaufmann M, et al. Cyclin B1 depletion inhibits proliferation and induces apoptosis in human tumor cells. *Oncogene*. 2004;23:5843–5852. doi: 10.1038/sj.onc.1207757.
13. Ouyang T, Bai RY, Bassermann F, von Klitzing C, Klumpen S, Miething C, et al. Identification and characterization of a nuclear interacting partner of anaplastic lymphoma kinase (NIPA). *J Biol Chem*. 2003;278:30028–30036. doi: 10.1074/jbc.M300883200.
14. Erbilgin A, Civelek M, Romanoski CE, Pan C, Hagopian R, Berliner JA, et al. Identification of CAD candidate genes in GWAS loci and their expression in vascular cells. *J Lipid Res*. 2013;54:1894–1905. doi: 10.1194/jlr.M037085.
15. Sekine Y, Hatanaka R, Watanabe T, Sono N, Iemura S, Natsume T, et al. The Kelch repeat protein KLHDC10 regulates oxidative stress-induced ASK1 activation by suppressing PP5. *Mol Cell*. 2012;48:692–704. doi: 10.1016/j.molcel.2012.09.018.
16. Silvestre-Roig C, de Winther MP, Weber C, Daemen MJ, Lutgens E, Soehnlein O. Atherosclerotic plaque destabilization: mechanisms, models, and therapeutic strategies. *Circ Res*. 2014;114:214–226. doi: 10.1161/CIRCRESAHA.114.302355.
17. Serre D, Gurd S, Ge B, Sladek R, Sinnett D, Harmsen E, et al. Differential allelic expression in the human genome: a robust approach to identify genetic and epigenetic cis-acting mechanisms regulating gene expression. *PLoS Genet*. 2008;4:e1000006. doi: 10.1371/journal.pgen.1000006.
18. Pinter SF, Colognori D, Beliveau BJ, Sadreyev RI, Payer B, Yildirim E, et al. Allelic imbalance is a prevalent and tissue-specific feature of the mouse transcriptome. *Genetics*. 2015;200:537–549. doi: 10.1534/genetics.115.176263.
19. Crowley JJ, Zhabotynsky V, Sun W, Huang S, Pakatci IK, Kim Y, et al. Analyses of allele-specific gene expression in highly divergent mouse crosses identifies pervasive allelic imbalance. *Nat Genet*. 2015;47:353–360. doi: 10.1038/ng.3222.
20. Ge B, Pokholok DK, Kwan T, Grundberg E, Morcos L, Verlaan DJ, et al. Global patterns of cis variation in human cells revealed by high-density allelic expression analysis. *Nat Genet*. 2009;41:1216–1222. doi: 10.1038/ng.473.
21. Bennett MR, Sinha S, Owens GK. Vascular smooth muscle cells in atherosclerosis. *Circ Res*. 2016;118:692–702. doi: 10.1161/CIRCRESAHA.115.306361.
22. Jones PD, Kaiser MA, Ghaderi Najafabadi M, McVey DG, Beveridge AJ, Schofield CL, et al. The coronary artery disease-associated coding variant in Zinc Finger C3HC-type containing 1 (ZC3HC1) affects cell cycle regulation. *J Biol Chem*. 2016;291:16318–16327. doi: 10.1074/jbc.M116.734020.

CLINICAL PERSPECTIVE

Despite the success of recent genome-wide association studies, there has been limited progress in understanding the function of the multiple risk loci identified. Here we have interrogated the functional effects of a coding variant in *ZC3HC1* that alters a conserved sequence in NIPA (Nuclear Interacting Partner of Anaplastic Lyphoma Kinase), a protein involved in cell cycle regulation. Allele-specific expression analysis in heterozygous carriers revealed preferential expression of the risk allele. Of note, the resulting amino acid change, arginine to histidine, at amino acid 363 in NIPA, results in important cellular changes. Thus, the protective variant exhibits increased phosphorylation of a critical serine residue, increased protein expression, and greater nuclear mobility. Excessive cell proliferation within the arterial wall is a key contributor to plaque growth. Here we show that the protective *ZC3HC1* variant was associated with lower rates of cell growth. Of note, the most robust GWAS signal for coronary artery disease is within *CDKN2BAS* at 9p21 and has been shown to alter expression of the *CDKN2B* and cellular proliferation. Other significant coronary artery disease loci, encompassing *PDGFD, MRAS*, and *KSR2*, also have documented roles in vascular smooth muscle cell growth. Taken together, these data support an important role for cell proliferation in atherosclerosis and its clinical consequences.

Circulation
Cardiovascular Genetics

Functional Validation of a Common Nonsynonymous Coding Variant in *ZC3HC1* Associated With Protection From Coronary Artery Disease

Tara Linseman, Sébastien Soubeyrand, Amy Martinuk, Majid Nikpay, Paulina Lau and Ruth McPherson

Circ Cardiovasc Genet. 2017;10:
doi: 10.1161/CIRCGENETICS.116.001498
Circulation: Cardiovascular Genetics is published by the American Heart Association, 7272 Greenville Avenue, Dallas, TX 75231

Print ISSN: 1942-325X. Online ISSN: 1942-3268

SUPPLEMENTAL MATERIAL

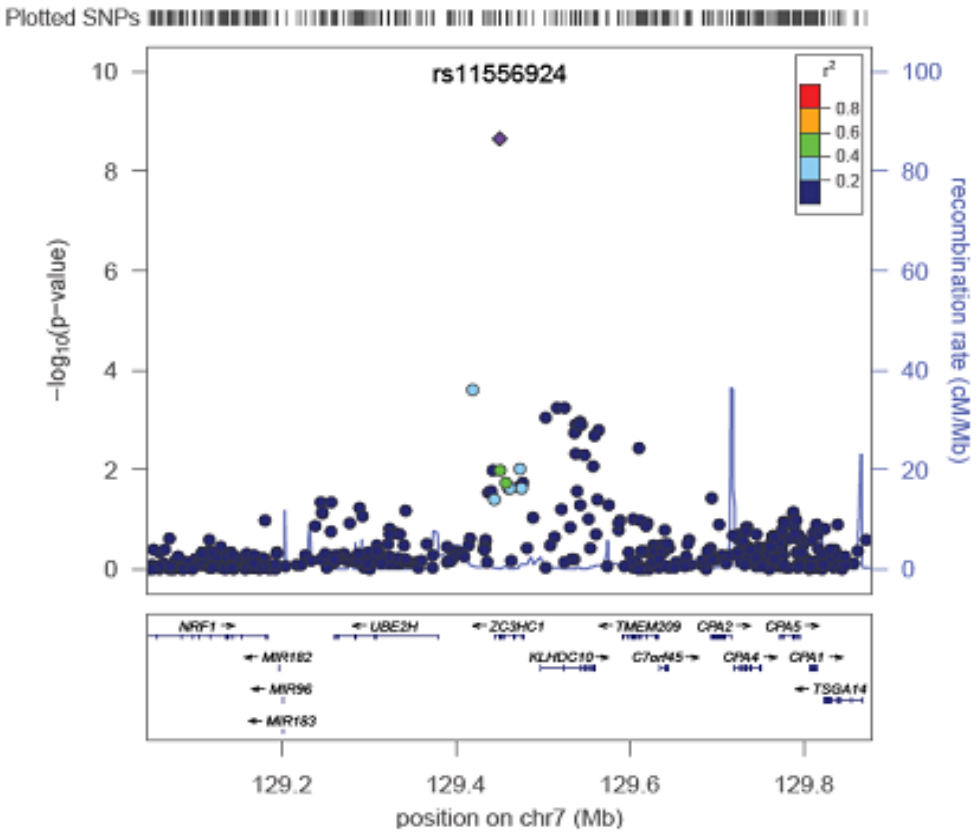

Figure S1. Local Disequilibrium plot of rs11556924. Plot of the NIPA locus derived from the 1000 Genomes project. No other SNP surrounding rs11556924 reached genome wide significance for its impact on CAD. rs11556924 is not in LD with neighboring SNPs.

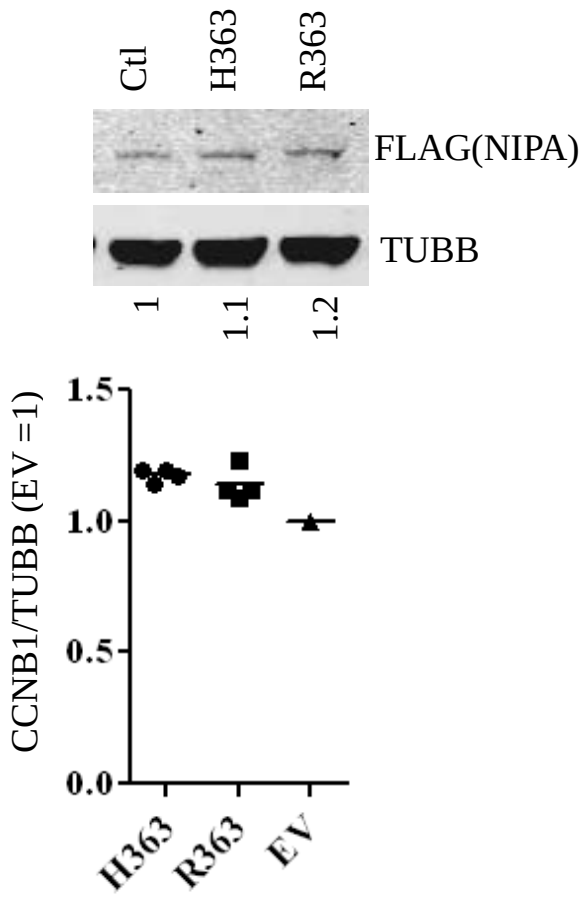

Figure S2. ***ZC3HC1*** **transfection induces mild CCNB1 upregulation**. Upon completion of the proliferation assay, lysates were analyzed by Western blotting with the indicated antibodies. Quantification of the blot is shown below (normalized to TUBB) while graphic represents 4 biological replicates and their mean. CCNB1 values are expressed relative to TUBB intensities and normalized to the empty vector (EV) values, set to 1. Error bars represent standard deviations. All changes are significantly different from the EV control (Student's 2-tailed t-test $p < 0.05$).

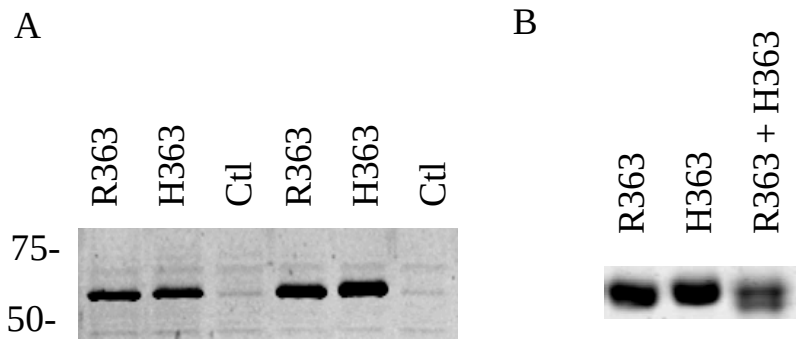

Figure S3. Greater retardation of the H363 variant by SDS-PAGE. A, NIPA is retarded by ~ 1 kDa on SDS-PAGE gel in HeLa cells. HeLa cells transfected with 0.5 or 1 ug of FLAG NIPA (or untransfected (Ctl)) were resolved by SDS-PAGE (4-15%), transferred to nitrocellulose and revealed with an anti NIPA antibody. B, GST NIPA (353-402) H/R363 forms fused to GST were resolved by SDS-PAGE (10%) and stained for protein using colloidal Coomassie blue.

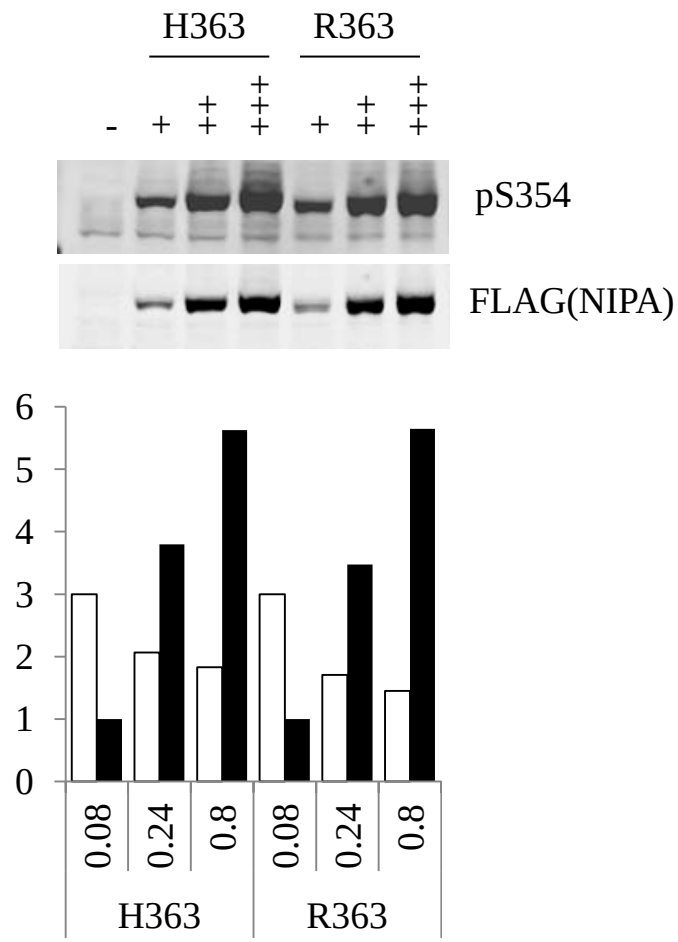

Figure S4. Extent of S354 phosphorylation is inversely correlated to its expression level in HeLa cells. Cells seeded in 12 well plates were transfected with indicated amounts of the FLAG-tagged NIPA constructs for 24 hours; S354 phosphorylation and NIPA levels were then assessed using a pS354 specific and a FLAG antibody, respectively. Bottom, quantification of relative phosphorylation (i.e. divided by the FLAG signal) for the blot above. Values are normalized to the matching H or R 0.08 sample (set to 3 for to simplify visualization). Data are representative of 2 biological replicates. Volume equivalents were loaded in each lane (~ 30 ug per lane).

TABLE S1. Nominally significant (p <0.05) epistatic interactions of rs11556924 with cell cycle regulatory genes

CHR	SNP2	OR_INT	STAT	P	q-value	lfdr	Marked Gene by SNP2
5	rs2069433	1.509	10.24	0.001	0.495	0.636	CCNB1
10	rs10906317	0.8079	10.03	0.002	0.495	0.666	MCM10
4	rs17009783	0.4003	9.959	0.002	0.495	0.677	MAD2L1
5	rs78658924	0.5405	9.353	0.002	0.495	0.786	PTTG1
5	rs73127323	1.445	9.275	0.002	0.495	0.802	CDK7
5	rs247265	0.8288	8.313	0.004	0.699	0.984	KIF2A
12	rs77619182	1.318	7.088	0.008	0.893	1	NUP37
12	rs35607042	1.876	6.656	0.01	0.893	1	NUP107
2	rs1050567	1.293	6.355	0.012	0.893	1	XPO1
5	rs7707035	0.8497	6.115	0.013	0.893	1	KIF2A
9	rs72758265	0.6487	6.033	0.014	0.893	1	CDC26
2	rs13384725	1.277	6.032	0.014	0.893	1	PSMD14
1	rs115564145	1.642	6.002	0.014	0.893	1	CENPL
10	rs139034306	1.326	5.856	0.016	0.893	1	BTRC
18	rs12956026	1.251	5.472	0.019	0.893	1	PSMG2
11	rs61893683	0.708	5.468	0.019	0.893	1	INCENP
2	rs1234375	0.5002	5.229	0.022	0.893	1	ORC4
20	rs17123673	0.713	5.22	0.022	0.893	1	MAPRE1
2	rs138541092	1.844	5.154	0.023	0.893	1	PSMD14
2	rs115432269	1.839	5.111	0.024	0.893	1	PSMD14
18	rs141702542	0.5312	5.046	0.025	0.893	1	CEP192
2	rs181662420	1.411	5.008	0.025	0.893	1	ALMS1
2	rs2018759	1.161	5.007	0.025	0.893	1	PSMD14
1	rs137903012	1.956	4.885	0.027	0.893	1	SDCCAG8
2	rs503664	0.8672	4.875	0.027	0.893	1	NOSTRIN
11	rs11236164	1.153	4.827	0.028	0.893	1	LIPT2(dist=90211),POLD3(dist=8609)
3	rs78916444	0.6402	4.751	0.029	0.893	1	STAG1
6	rs2307323	0.5168	4.748	0.029	0.893	1	MCM3
20	rs148847980	0.5129	4.724	0.03	0.893	1	CEP250
17	rs192985617	0.6034	4.698	0.03	0.893	1	SKA2
5	rs152204	1.146	4.639	0.031	0.893	1	IPO11
12	rs2471533	1.31	4.562	0.033	0.893	1	CEP290
3	rs13077681	1.62	4.466	0.035	0.893	1	GORASP1
17	rs11657745	0.7073	4.349	0.037	0.893	1	SKA2
5	rs16890800	0.8781	4.235	0.04	0.893	1	IPO11
14	rs8016207	1.19	4.172	0.041	0.893	1	PPP2R5C
1	rs3218203	1.18	4.151	0.042	0.893	1	E2F2
9	rs112610512	1.806	4.147	0.042	0.893	1	CDK5RAP2
4	rs3811740	0.8716	4.135	0.042	0.893	1	PLK4
2	rs16835779	0.5466	4.131	0.042	0.893	1	ORC2
20	rs6107051	0.6973	4.121	0.042	0.893	1	NINL
5	rs16893963	0.6116	4.033	0.045	0.893	1	CENPK
11	rs11236187	1.136	4.005	0.045	0.893	1	POLD3(dist=10461),CHRDL2(dist=42908)

18	rs34183067	1.217	3.999	0.046	0.893	1	CEP76,PSMG2
3	rs6789152	1.148	3.977	0.046	0.893	1	STAG1
1	rs76225126	1.482	3.976	0.046	0.893	1	ITGB3BP
9	rs62574668	0.514	3.942	0.047	0.893	1	CENPP
2	rs147393308	1.344	3.907	0.048	0.893	1	ORC4
1	rs72679056	1.477	3.885	0.049	0.893	1	ITGB3BP

Expanded Methods

Cell treatments

Cells were transfected either with Fugene 6 (Promega) or GenJet II (Signagen) using 3:1 reagent to DNA ratios while silencing was performed with RNAimax (Thermo Fisher Scientific).
For HUVECs and VSMCs, infectious particles were added to cells in the presence of 4 µg/ml polybrene. Viral particles were obtained by cotransfection of 293FT cells (Thermo Fisher Scientific) with PLVX plasmids, either empty or harboring FLAG-NIPA, together with pPAX2 and pMDG2.

Cell lysis for Western blotting

Cells were lysed in buffer A (20 mM HEPES, 130 mM NaCl, 1 mM EDTA, 1% TRITON X-100, pH 7.4 supplemented with phosphatase and protein inhibitor cocktails (PhoSTOP and EDTA-free cOmplete protease inhibitors, Roche)) for 5 min on ice. For endogenous NIPA detection, a fractionation enrichment approach was elected to address the weakness of the signal. Cells were lysed in a low salt buffer (10 mM HEPES, 10 mM KCl, 0.1% NP40, pH 7.4), centrifuged, and the residual cellular material containing NIPA was recovered in RIPA buffer (50 mM Tris-HCl, 150 mM NaCl, 1% TRITON X-100, 0.5% NaDeoxycholate, 0.1% SDS, pH 8.0; supplemented as above) and sonicated briefly. Lysates (~ 30 µg) were cleared by centrifugation, heated at 95 ºC under reducing conditions in SDS-PAGE sample buffer and resolved by SDS-PAGE gels (8 or 10%). Proteins were then transferred to nitrocellulose membranes which were then incubated in Odyssey blocking buffer for 1 h prior to antibody

addition. All primary antibodies were used at 1:2,000 dilutions while secondaries (LICOR) were used at 1:20,000. Dilutions and washes (4 x 5 min after each antibody incubation) were performed in PBS. Incubations were performed for 16 h or 1 h for primary and secondary antibodies, respectively. Antibodies are listed in the supplementary Materials and Methods section. Images were acquired on a LI-COR Odyssey system. Quantifications were performed using the Odyssey system application software using local median average (Top and bottom signals).

Cloning and expression constructs

For immunocytochemical experiments, *ZC3HC1* was cloned C-terminal to pEYFP or pECFP as indicated. For general protein expression, NIPA was expressed with an N terminal FLAG tag from either pCDNA3 or pCMVTag2. pCDNA FLAG-NIPA (R363) was obtained from Dr. Florian Basserman (München, DE). To measure relative expression levels, an internal ribosome binding site driving eGFP was introduced in pCMVTag2NIPA. For experiments involving viral infection, FLAG-NIPA was transferred to a lentiviral expression vector PLVX (Clontech). pCMX/Cyclin B1(17) was a gift from Jonathon Pines (Addgene plasmid # 26060) [1]. SKP1 cDNA was derived from HepG2 cells mRNAs and sub-cloned in pGEX-4T-1 (GE Healthcare). GST-NIPA353-402 was kindly provided by Dr. Lena Illert (Freiburg, DE). GST fusion proteins were expressed in the BL21 *E. Coli* strain. Point mutations were introduced by QuikChange mutagenesis (Agilent). All constructs were verified by sequencing.

1 Hagting, A., Jackman, M., Simpson, K. and Pines, J. (1999) Translocation of cyclin B1 to the nucleus at prophase requires a phosphorylation-dependent nuclear import signal. Curr. Biol. **9**, 680–9.

Supplemental Materials

Antibodies:

Primary:

Tubulin beta: GTX11307 (GeneTex)

CCNB1: SC-594 (Santa Cruz Biotechnology)

GFP: G1544 (Sigma-Aldrich)

FLAG: F3165 (Sigma-Aldrich)

NIPA: 4497 (Cell Signaling)

NIPA pS354: ab63557 (Abcam)

Secondary (LI-COR):

IRDye 800CW Donkey anti-Mouse

IRDye 680LT Donkey anti-Rabbit

siRNA (sense sequence shown):

NIPA: GGAGAUAGCUGGAAUGAGAUU

NT: Negative control #1 (NT#1); Life Technologies

qPCR oligonucleotides :

PPIA:

ACCGTGTTCTTCGACATTGC

TTCTGTGAAAGCAGGAACCC

NIPA:

TTTGAAAAATTAAGGCTGAGTTC

AATCCCACACTCCTTTAACAGAAC